Atmospheric Research 270 (2022) 106047

Contents lists available at ScienceDirect

Atmospheric Research

journal homepage: www.elsevier.com/locate/atmosres

On the relationship between lightning superbolts and TLEs in Northern Europe

Andrea Pizzuti [a,b,*], Alec Bennett [a,b], Serge Soula [c], Samir Nait Amor [d], Janusz Mlynarczyk [e], Martin Füllekrug [a], Stéphane Pédeboy [f]

[a] Department of Electronic and Electrical Engineering, University of Bath, Bath, UK
[b] Bristol Industrial and Research Associates Limited (Biral), Portishead, UK
[c] Laboratoire d'Aérologie, Université de Toulouse, CNRS, OMP, UPS, Toulouse, France
[d] Centre de Recherche en Astronomie, Astrophysique et Géophysique, Division Physique Solaire, Algiers, Algeria
[e] Department of Electronics, AGH University of Science and Technology, Krakow, Poland
[f] Météorage, Pau, France

ARTICLE INFO

Keywords:
Superbolt
Lightning
TLEs
Atmospheric electricity
Natural hazards

ABSTRACT

Lightning occurrence at higher latitudes in northwestern Europe is by far less frequent than mainland continental and the Mediterranean during most of the year. Yet, as recent studies suggest, this region harbors a large fraction of the most energetic lightning flashes on Earth, commonly referred to as superbolts. In this study, we examine the time/locations of intense cloud-to-ground (CG) strokes (>200 kA in absolute value), provided by Météorage for the 10.5-year period (from Jan 2010 to Jul 2020), to present a high-resolution map of their distribution, pointing out relevant discrepancies observed between -CG and + CG, respectively. We additionally investigate the potential of superbolts to result in short-lived optical phenomena above thunderstorms, collectively known as transient luminous events (TLEs). Observations in the region indicate that isolated superbolts with substantial charge moment change can produce sprites during low active marginal winter thunderstorms, in the absence of concurrent IC/CG activity several minutes before and after the event. An example is described when 3 sprites were captured in a similar context during the night of 7th/8th February 2016. We suggest that: i) convergence and aerosols advection from sea surface and busy shipping lanes may favour deep convection and cloud electrification on the English Channel with respect to surrounding areas. Inherent differences in cloud charge structure of sea based storms could lead to faster negative leader vertical velocity than those for storms over land, on average, and hence in larger peak currents, determining the winter peak of negative superbolts in the area; ii) areas occupied by the most populated superbolt clusters can be used to conduct future research in the region, aimed at better characterising microphysical properties of superbolts and their potential in generating TLEs.

1. Introduction

The term "superbolt" was first introduced by Turman (1977) to identify rare and extreme lightning strokes observed by optical sensors on board of the Vela satellites, characterised by optical power of at least 100 GW (i.e. 100 times or more than median value) and found to occur mostly in the coastal areas near Japan and over the northern Pacific Ocean. Since then, however, a long debate has been sparked about whether superbolt designated events were related with a specific class of powerful lightning or an undiscovered exotic lightning process, or if merely the result of a measurement bias. Combining radio frequency (RF) and optical data from FORTE (Fast On-Orbit Recording of Transient Events), Kirkland (1999) found that the brightest events recorded, falling within the range of peak optical power given by Turman (1977), were globally distributed and mostly associated with both negative and positive cloud-to-ground (CG) strokes, exhibiting peak current values comparable on average to those associated with common lightning strokes. This finding, along with the absence of any unique VHF emission, led Kirkland to suggest that superbolts were simply powerful optical pulses originating from typical lightning strokes but occasionally detected by the satellite instruments along unobscured line of sight to the lightning channel. Yet, a more recent 12-years analysis of FORTE

* Corresponding author at: Department of Electronic and Electrical Engineering, University of Bath, 2 East, BA2 7AY, Bath, United Kingdom.
E-mail address: ap2423@bath.ac.uk (A. Pizzuti).

https://doi.org/10.1016/j.atmosres.2022.106047
Received 20 October 2021; Received in revised form 6 January 2022; Accepted 20 January 2022
Available online 26 January 2022

observations by Peterson and Kirkland (2020) indicates that only the upper optical power range (≥ 350 GW), largely dominated by intense +CG strokes, should be regarded as a distinctive class of superbolt-lightning, while other less bright events (~100 GW) result from normal lightning, observed under favourable viewing conditions and would not be recognized as such by a different observer elsewhere. Furthermore, the global distribution of superbolt activity exhibits a clear asymmetry in the two cases, with weaker events distributed in the ordinary tropical lightning hotspots while larger optical powers exceeding 350 GW showing similarity with previous results from Turman (1977), being highly concentrated in oceanic thunderstorms, and in particular at the mid-latitudes of Mediterranean Sea, the Sea of Japan and the North Pacific during the winter season. Winter thunderstorm dynamics in such areas enhances the production of strong +CG strokes associated with transient luminous events (TLE) activity (Takahashi et al., 2003; Hayakawa et al., 2004; Yair et al., 2015), suggesting the possibility that the brightest events identified by Peterson and Kirkland (2020) may occasionally precede TLEs development. Observations from the LSO (Lightning and Sprite Observations) experiment, on board of the International Space Station (ISS), additionally provided early examples of optical superbolt-TLE composite images (Blanc et al., 2007).

Instead of using the optical energy as measured from spaceborne instruments, Holzworth et al. (2019) have given a different definition of superbolt based on RF emission in the VLF (5 to 18 kHz) from CG strokes recorded by the WWLLN global lightning network. A superbolt is hence classified as such if it exceeds 1 MJ stroke energy, which is about 3 orders of magnitude above the mean. WWLLN stroke energies are estimated by integrating the *E*-field through the VLF sferic waveform and the resultant radiated stroke power is found to be empirically proportional to the stroke peak current, normally provided by other lightning networks (Hutchins et al., 2012). The global distribution of these sources for 2010–2018 remarkably differs from the location of tropical lightning chimneys in Africa, Southeast Asia and South America, confirming the location bias previously noticed for optically detected superbolts and showing the highest concentrations in the eastern North Atlantic, the Mediterranean, and over the Andes Mountains in South America. In addition, Holzworth et al. (2019) found that superbolt activity is preferentially recorded between November and February, during the northern hemisphere winter. A recent study by Ripoll et al. (2021) reported electromagnetic (EM) measurements from both ground and space relatively to some of WWLLN superbolts detected in Europe, establishing the exceptional nature of these sources and revealing they also leak significantly larger VLF radiation into space than typical flashes.

Here, we provide a detailed analysis of superbolt activity in the region of northwestern Europe highlighted by Holzworth et al. (2019), that includes the British Isles and the North Sea. Following the criteria by Yair et al. (2020), we examine 10.5-year (2010−2020) of lightning data obtained from the French national operational LF lightning location system (LLS) (Météorage), defining as superbolts the negative and positive CG strokes, whose peak current amplitude is larger than 200 kA in absolute value. The corresponding coordinates are later processed with the DBSCAN (Density-Based Spatial Clustering of Applications with Noise) algorithm to identify the dominant superbolt clusters, and additional timing information also allows their temporal and seasonal distribution to be characterised. Combined ground-based optical and EM observations of TLEs in the same region are hence used to investigate the link with superbolts, especially during wintertime when this part of Europe experiences meteorological conditions like those in Japan (Takahashi et al., 2003; Adachi et al., 2005).

The paper is organized as follows: in section 2 we describe the type of data and analysis methods used in this study; in section 3 we present our results, providing a comprehensive spatial/temporal overview of superbolt distribution in the study domain and describing a peculiar case of sprite-producing superbolts during a marginal winter thunderstorm in the UK; in section 4 we discuss our results, giving some ideas to advance knowledge; finally, in section 5 we summarizes the main conclusions.

2. Data and methods

The data of this study cover the period ranging from January 2010 to July 2020 and extend over an area delimited approximately between (48°N, 60°N) in latitude and (12°W, 8°E) in longitude. This domain falls within the range of Météorage LLS, which is based on a network of Vaisala LS7002 sensors, working in the LF band 1–350 kHz. Each sensor measures the EM signal emitted by both CG and intra-cloud (IC) lightning stroke activity. Multiple detections of the same event are combined by applying magnetic direction finding and time-of-arrival techniques to provide accurate information for each stroke as the occurrence time, latitude, longitude, the peak current amplitude with polarity and the type (IC/CG). The effective range of Météorage encompasses all of Europe area and part of the North Atlantic Ocean, as a result of the collaboration with EUCLID (European Cooperation for Lightning Detection). Pédeboy et al. (2018) reported a detection efficiency of 97% and 56% for CG and IC flashes, respectively, with the corresponding median location accuracy of 100 m and 1.64 km, respectively. The stroke peak current, used in the superbolt definition, is estimated from the magnetic field remotely detected by the sensors. A transmission line model is used to convert the measured EM fields to lightning current in the return stroke (RS), assuming a constant propagation speed. However, since this speed is not fixed but varies, an error is committed on the peak current calculation. Peak current estimates are calibrated with direct current measurements of triggered lightning or at instrumented towers and are validated with a median absolute accuracy of the order of 15–20% for negative CG subsequent RS (Schulz et al., 2016). Larger uncertainty remains about the peak current estimate of first negative RS, positive RS and intra-cloud IC discharges, as no direct validation method is currently available. Despite such large uncertainties in the peak current absolute magnitude, values larger than 200 kA are certainly indicative of a particular class of lightning, corresponding in general to less than about 0.15–0.05% of total lightning CG strokes recorded.

We use additional simultaneous EM measurements in the ELF-VLF band to further characterise the TLE parent CG properties, previously identified by Météorage. These include: 1) quasi-electrostatic currents in the ELF range 1–45 Hz, recorded at 2 different sites in southern UK using the technique proposed by Bennett (2013, 2017); 2) ELF magnetic field recordings performed at Hylaty (Poland), processed to reconstruct the current moment waveform (CMW) and estimate both the charge moment change (CMC) and the impulsive CMC (iCMC) of sprite parent +CG strokes (Kulak et al., 2014; Mlynarczyk et al., 2015); 3) two high frequency magnetic induction coils detectors operating in the range 0.1–50 Hz and installed at the Eskdalemuir Geophysical observatory in Scotland (Beggan and Musur, 2018); 4) Very Low Frequency (VLF) recordings at Algiers, Algeria (36.45°N, 3.28°E) to monitor VLF transmission signal perturbations for evidence of lightning-ionosphere coupling effects associated with TLEs and superbolts (NaitAmor et al., 2010).

Cloud Top Temperatures (CTT) are issued from the thermal infrared band (IR) at ~11–13 μm of the Spinning Enhanced Visible and Infrared Imager (SEVIRI) onboard the Meteosat Second Generation (MSG) satellite operated by the European Organization for the Exploitation of Meteorological Satellites (EUMETSAT). The radiometer SEVIRI scans the Earth disk within about 12 min, from east to west thanks to the satellite rotation and from south to north thanks to the rotation of a scan mirror (Aminou et al., 1997). It provides images in 12 spectral bands every 15 min. The spatial resolution for the thermal channel is 0.027°, which corresponds to 3 km at the subsatellite point and about 4.5 km at the latitude of the study area. The study area is therefore scanned four times in one hour, and around 10, 25, 40 and 55 min of each hour. The accuracy of the CTT values depends on several parameters, as the type of clouds, the time during the day, the geographical location around the Earth. In the study by Taylor et al. (2017), that compared SEVIRI cloud top temperatures from the new CLAAS-2 (CLoud property dAtAset using SEVIRI, Edition 2) dataset against Cloud-Aerosol Lidar with Orthogonal

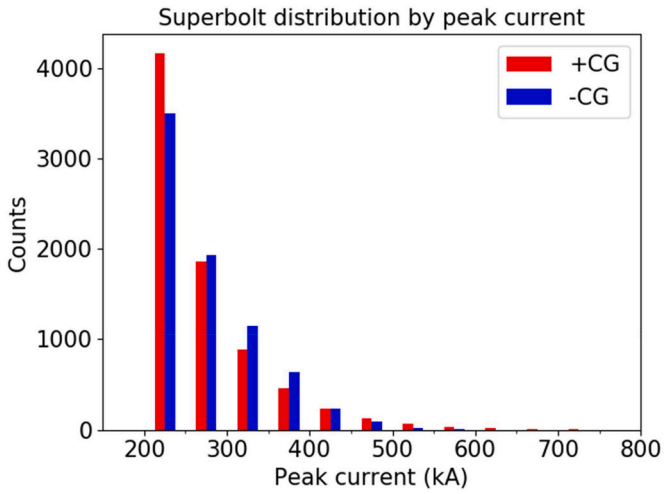

Fig. 1. Histogram showing the superbolt (>200 kA in absolute value) distribution by peak current and polarity. The median peak current is about 250 kA for both +CG and -CG, respectively.

Polarization (CALIOP) data, the error was lower than 2–3 K in UK.

Optical observations of TLEs and particularly sprites in the same spatial domain are coincidentally obtained by low light CCD cameras with a standard PAL frame rate of 25 fps, operated in trigger mode by networks of citizen scientists and more recently by the University of Bath (UK). The timestamps of TLEs videos in the observation database has been thus matched with the superbolt list to identify and locate the large peak current parent stroke.

All the spatial statistics are computed using 0.25° × 0.25° grid cells, each cell corresponding to dimensions of approximately 28 km by 18 km at 50°N. The superbolt density is obtained as the ratio of the total number of events in a grid cell and the area of the grid cell, expressed as flashes per square kilometre (fl km^{-2}). In addition, an accurate idea of the spatial shape of the data distribution is produced by applying the kernel density estimation (KDE), which produces an estimate of the probability density distribution which that data is drawn from, as a weighted sum of Gaussian distributions. We also applied KDE to determine diurnal patterns of superbolt activity. This is done after reprocessing the lightning data into 1-h width counts of superbolts by season (DJF, MAM, JJA, SON).

Individual superbolt location processing into clusters is achieved by applying the DBSCAN algorithm (Ester et al., 1996; Kriegel et al., 2011). DBSCAN was chosen as the clustering algorithm mainly for its capability to handle noise, no requirement to specify the number of clusters and the arbitrary cluster shapes. DBSCAN clusters *n*-dimensional points based on the radius that defines a circular neighbourhood (*epsilon*) around each point and the minimum number of points necessary to form a cluster (*MinPoints*) (Kriegel et al., 2011). In the context of DBSCAN, each point in the data set is classified as: 1) a core point of a cluster, if there are at least *MinPoints*-1 other points in its neighbourhood; 2) an edge point, if it is within the radius of a core point yet does not satisfy the minimum samples requirement; 3) noise, if it does not contain the minimum number of samples and it is not within the radius of a core point. Since the two parameters are domain-dependent, their optimal choice is not known a-priori but must be manually tuned, using domain-specific knowledge related to the problem at hand. In this case, the identification of a core point requires a neighbourhood search radius *epsilon* = 25 km (i.e. well above the lightning location error and larger than the

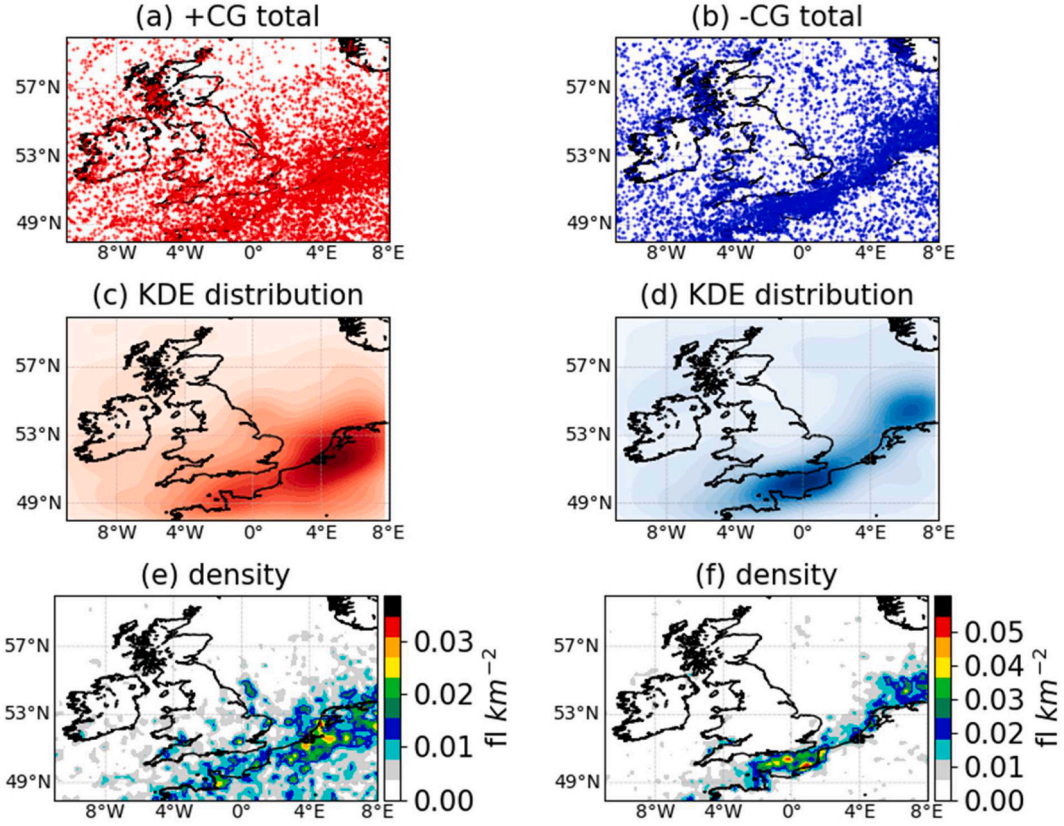

Fig. 2. Overall distribution of Météorage superbolts by polarity for the study area: (a,b) scatter plot of superbolt coordinates; (c,d) corresponding probability density plots (0.25° resolution), determined using the kernel density estimation (KDE); (e,f) superbolt flash density map, calculated adopting a spatial resolution of 0.25°x0.25° and smoothed by a.
Gaussian filter for clarity.

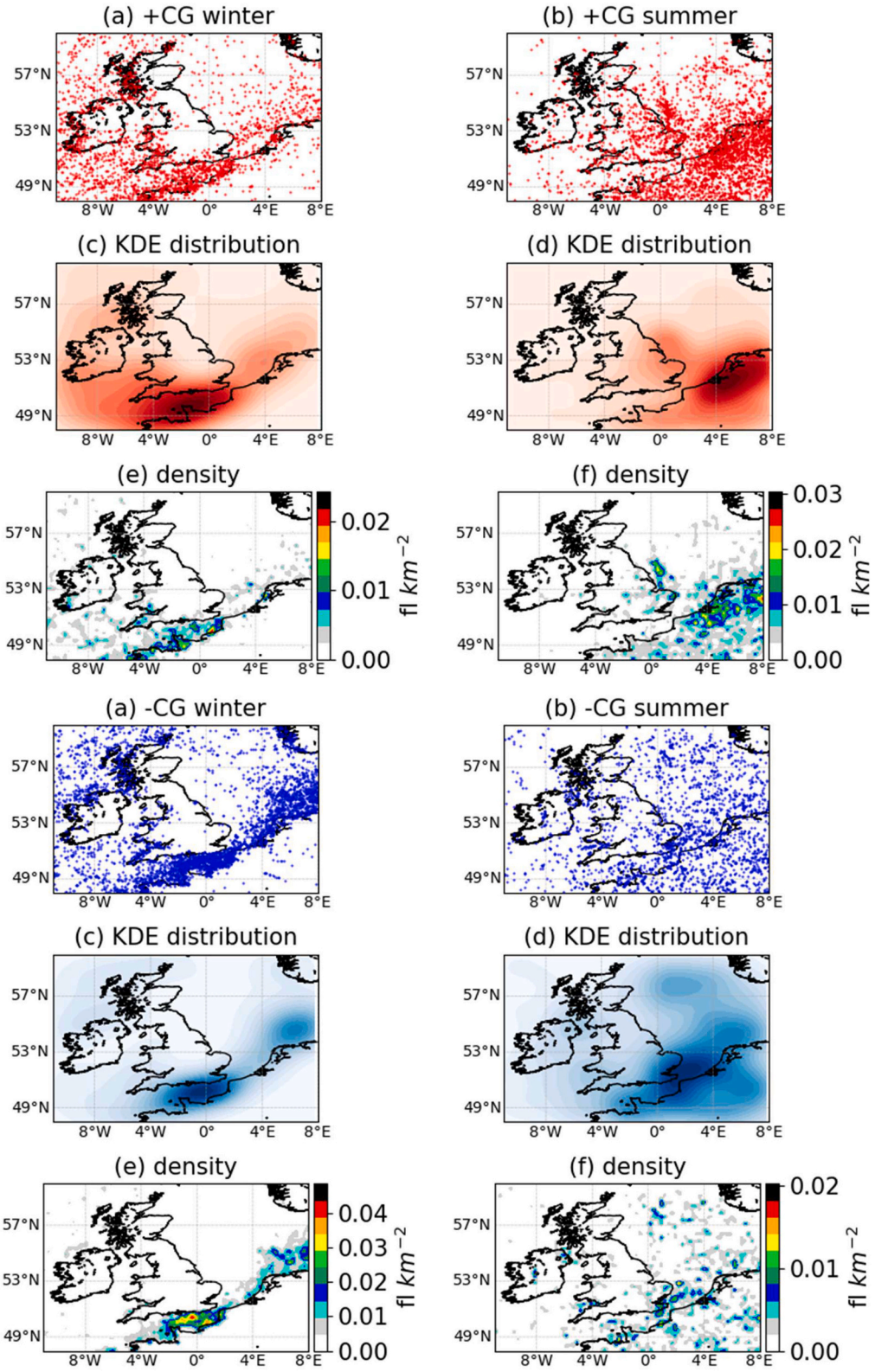

Fig. 3. A.Overall distribution of Météorage positive superbolts during winter (NDJF) and summer (MJJA) months: (a,b) scatter plot of superbolt coordinates; (c,d) corresponding probability density plots (0.25° resolution), determined using the kernel density estimation (KDE); (e,f) superbolt flash density map, calculated adopting a spatial resolution of 0.25°x0.25° and smoothed by a Gaussian filter for clarity.
3B. Overall distribution of Météorage negative superbolts during winter (NDJF) and summer (MJJA) months: (a,b) scatter plot of superbolt coordinates; (c,d) corresponding probability density plots (0.25° resolution), determined using the kernel density estimation (KDE); (e,f) superbolt flash density map, calculated adopting a spatial resolution of 0.25°x0.25° and smoothed by a Gaussian filter for clarity.

(a)

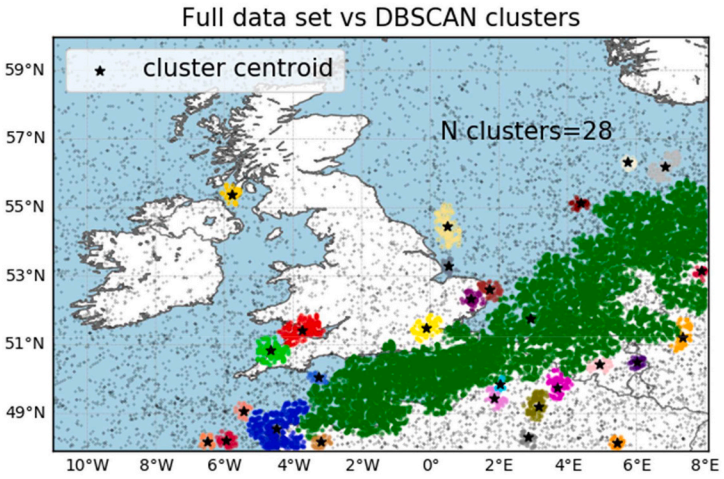

(b)

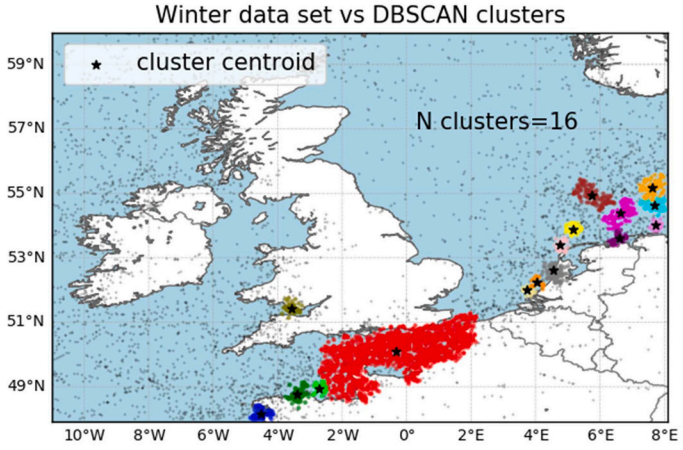

(c)

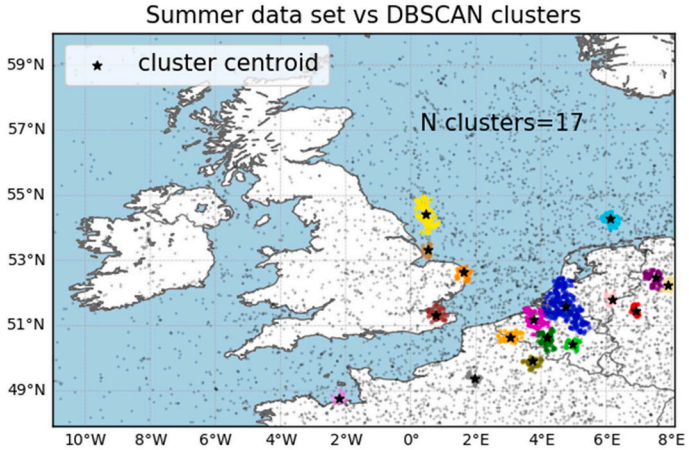

Fig. 4. Superbolt lightning clusters identified with the DBSCAN algorithm on the (a) full and (b,c) seasonal data set, respectively. Each cluster is distinguished from the other by using different colours for its elements. The black solid star indicates the centroid of the cluster.

typical size of single-celled systems in the UK) and a minimum number of neighbours *MinPoints* = 25 strokes. This choice produces results that are consistent with previously defined density maps, while limiting the influence of individual localized thunderstorms generating superbolts on the clustering process that would increase by setting smaller radii and number of strokes. On the other hand, a larger *epsilon* would produce coarser resolution, masking eventual features such as the observed contrast along coastlines for a given stroke polarity.

3. Results

3.1. Regional distribution of superbolts

During the 10.5-year period considered, Météorage detected a total of 7578 negative and 7858 positive intense CG strokes (>200 kA in absolute value) across the study area. Fig. 1 shows their peak current distribution by polarity, indicating a similar absolute median value of about 250 kA. This value is comparable to the mean (−267 kA) found by Holzworth et al. (2019) for the limited subset of superbolts identified by WWLLN over continental United States that matched with the corresponding large negative strokes located by ENTLN. Such extreme events are relatively rare if compared to the total number of CG strokes recorded. Pedeboy et al. (2017) estimated an average occurrence rate of about 0.18% of the overall CG activity recorded by EUCLID in Western Europe for 2007–2016 period. Yet, the relative proportion of intense CG strokes is found to exhibit significant differences on a regional and seasonal basis.

Here such spatial and temporal patterns are discussed in greater detail with respect to the previously defined domain. Fig. 2 presents the overall plot of all the 15,436 large strokes broken into two colours by polarity. From Fig. 2 (a, b) early evidence is seen of a location bias between powerful +CGs, which appear more scattered across the domain, and -CGs which are preferentially found on the sea and exhibit a sharp contrast on the coastlines. This geographical pattern of strokes of different polarity is much clearer in Fig. 2 (c,d), showing the related probability density estimated with 0.25° spatial resolution over the entire domain using the KDE algorithm. The core activity of positive superbolts is found on land, over the border between Belgium and the Netherlands, reaching a maximum density of about 0.04 fl km^{-2} (Fig. 2e). By contrast, the main negative cores are observed on the English Channel and off the Dutch coast, with a maximum of 0.06 fl km^{-2} (Fig. 2f). A slight increase in activity in both polarities can be also seen on the West coast of Scotland and Northern Ireland, where convection may be enhanced by the steep slopes of coastal mountains. Yet, an even more remarkable discrepancy is noticed when also including the winter/summer seasonal pattern, as seen in Figs. 3A and 3B. The strong -CGs essentially occur on the sea surface during the winter season (NDJF), with the highest density found across the English Channel (~0.05 fl km^{-2}). The winter -CG core tends to overlap with the +CG one, which shows a consistent shift westward with respect to the summer months (MJJA). Winter lightning outbreaks are generally associated with deep North Atlantic low-pressure systems, characterised by high pressure gradients and strong winds, which move unstable cold and moist polar maritime air over relatively warmer sea surface temperatures (as opposed to the cold land) into the region of study. In this context, instability and lightning potential is enhanced, especially in the western side of the domain, by the contrast with warmer North Atlantic current and by the orography, which forces air to lift for example near mountainous terrain of western Scotland and Wales. Alongside the calculation of density maps, the spatial data set is reduced into local superbolt clusters by applying the DBSCAN algorithm to their coordinates. The identified clusters and the relative centroids are plotted in Fig. 4. By considering the full data set, irrespective of the stroke polarity, 28 clusters are localized, the largest of which is centred on the eastern side of the Strait of Dover and encompasses an area that extends from the English Channel to the North Sea, mostly delimited by the coastline

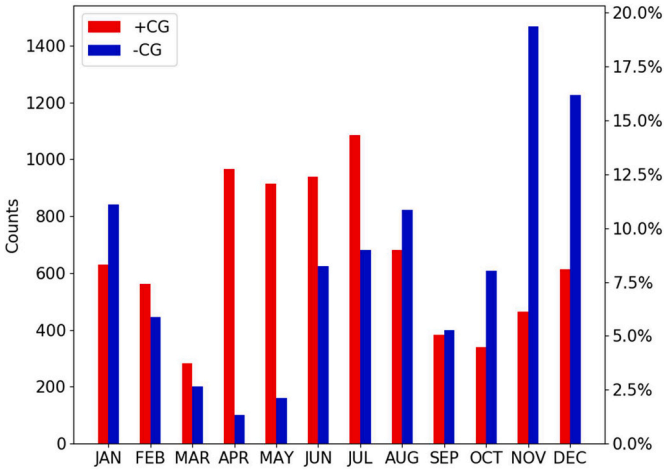

Fig. 5. Monthly distribution and relative percentage of superbolts by polarity.

(Fig. 4a). Other relevant local clusters include the Bristol Channel and Brittany. Looking at specific seasons, however, the seasonal shift in cluster locations is further confirmed, showing that summer activity is more evenly distributed and the largest summer cluster on land in Belgium is significantly less populated than the winter peak cluster on the English Channel (Fig. 4b and c).

Fig. 5 introduces the annual variation of superbolt activity in the study area. The monthly absolute distribution and the relative percentage compared to the total with respect to the polarity indicate an overall peak in negative superbolts in November and December, when the number of events is about 2 times larger than summer months (JJA) and up to 14 times with respect to spring (MAM). Looking at the whole year, the months November–February account for more than 52% of all negative superbolts. Additionally, the analysis shows that positive superbolts follow a similar annual trend during most of the year but, differently, tend to occur more often during spring and summer time (April to July) with a secondary and smaller amplitude peak between December and January.

Such finding suggests that superbolts are preferentially produced in the transition periods before summer and winter, which can be explained by different thunderstorm characteristics related to the changing general synoptic patterns of thunderstorms producing superbolts. Additional indications in this sense can be obtained by observing the diurnal distribution of these intense lightning strokes during different seasons. This is summarized in Fig. 6, displaying the probability density distribution of superbolts using the KDE method by hour of day and polarity. Autumn and Winter show the closest similarity, with -CGs exhibiting a clearly bimodal distribution and dominating during the early morning on +CGs, which conversely remain almost constant throughout the day and exceed negative stroke activity during the late morning and early afternoon. The diurnal variations observed are not in phase with land-based convection but more likely to be marine-based, as the stroke locations previously confirmed. The ~04 UT peaks in marine activity may also be related to the time of maximum wintertime land-sea temperature difference and corresponding land-breeze convergence. Differently, the maximum annual peak in +CG occurs during Spring/Summer season, with greatest activity during the afternoon. This seasonal peak occurs when stroke locations are mostly distributed on continental mainland, where convection initiated by solar heating of the land is important. Negative Spring superbolts activity shows a similar double peak in diurnal variation as for positive, but the afternoon amplitude is less pronounced. This is consistent with the suggestion that land-based thunderstorms initiated by afternoon solar heating are more likely to produce positive superbolts than negative ones.

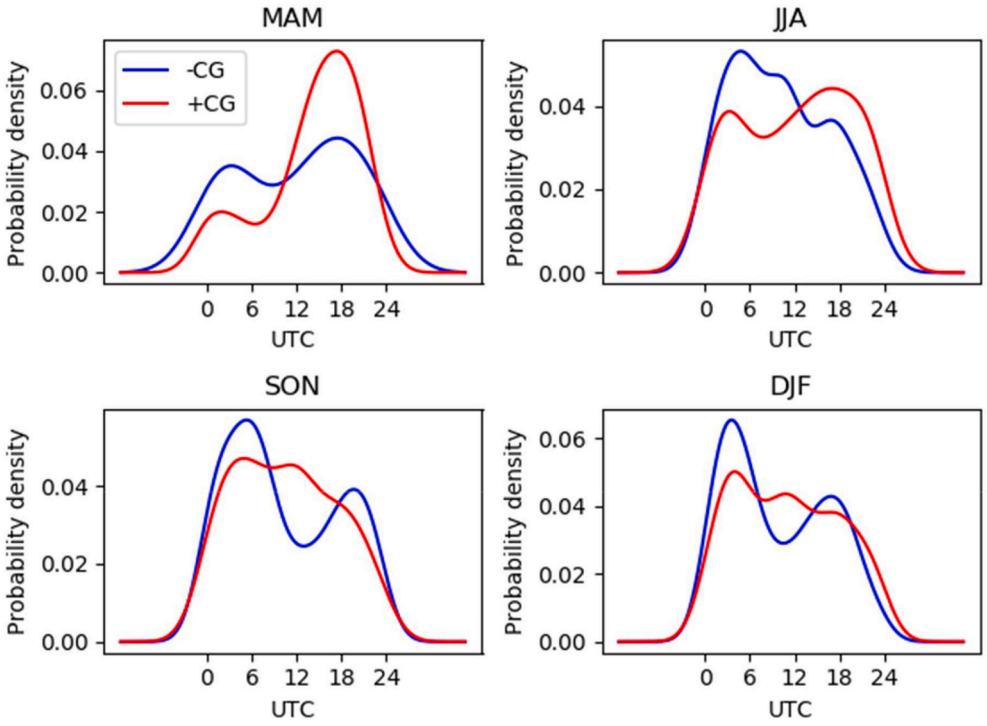

Fig. 6. Diurnal probability density of superbolts based on 2010–2020 data by season, estimated with KDE.

3.2. TLEs observations and superbolts in northern Europe

Particularly intense lightning, such as cloud-to-ground (CG) lightning discharges with large charge moment change (CMC) and occasionally very high peak current as superbolts, can produce short lived optical emissions above thunderclouds, among which sprite-halos and elves are the most commonly observed (Pasko, 2010 and references therein; Pasko et al., 2012). The mechanism of TLE formation is now well established, but extensive research on their microphysical properties is still ongoing (i.e. for example, to explain the rich variety of sprite morphologies). The occurrence of TLEs across Europe mirrors the lightning density distribution and peaks at summer on continental mainland (Arnone et al., 2020). Autumn and winter TLEs activity is generally lower and concentrated on the Bay of Biscay and over the coastal areas of the Mediterranean Sea in southern Europe and the Middle East.

The areas of northern Europe that include British Isles and North Sea generally experience significantly less thunderstorms (up to 10 times) than the rest of Europe (Anderson and Klugmann, 2014). The knowledge about TLEs occurrence in this area is relatively scarce. Optical observations at higher latitudes in northern Europe presents the basic problem of barely dark skies during summer, when most northern European thunderstorms occur. TLEs observations (1 sprite,1 elve) on the Baltic Sea have been reported by Mäkelä et al. (2010) and represented the northernmost European TLEs until then. Arnone et al. (2020) indicated a total of 25 additional TLEs observed (24 sprites, 1 bluejet) in 2009–2013 in the same area. A single column sprite was later recorded in 2018 by the cameras of project Hessdalen even further north at a latitude of approximately 63° along the coast of Norway. The EM signal of the parent +CG was analysed by Pizzuti et al. (2021) and showed a peak current of 163 kA and a total charge moment change (CMC) of 1750C km.

The geographical domain considered in this study is partially covered by cameras operated by the UK Meteor Network (UKMON) and NEMETODE (Network for Meteor Triangulation and Orbit Determination). As these are primarily set up for meteor observations, recording of TLEs is serendipitous and rare. Nevertheless, citizen scientists recorded some tens of sprites in the area during 2010–2020. More recently, a new low-light and high-resolution charge-coupled device (CCD) camera (Watec 902H2) mounted on a fixed tripod and remotely controlled, was installed in 2019 at the University of Bath (UK) and specifically configured for capturing TLEs across the English Channel. The system has been already successful at detecting the first ever ELVE from the UK (Fig. 7). The donut-shaped optical emission was produced by the electromagnetic pulse (EMP) of an extreme -CG stroke (−750 kA) on the NW coast of France.

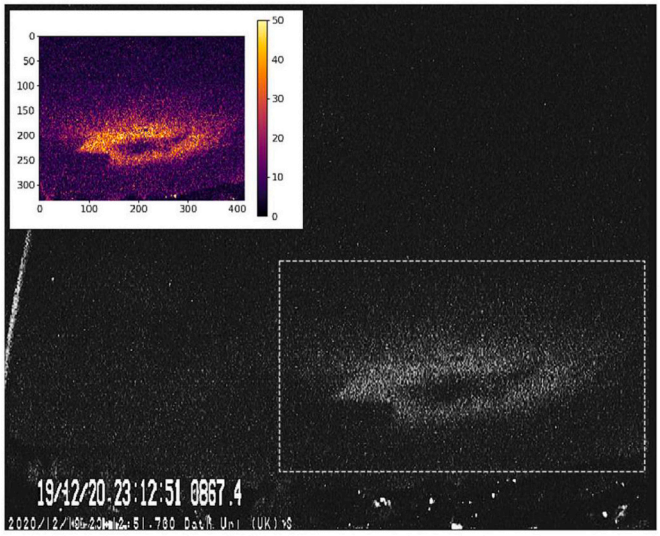

Fig. 7. The first ever elve detected from the UK on a low-light camera installed at the University of Bath. The CG stroke (−750 kA) responsible of this optical emission on the lower ionosphere was located close to the NW coast of France (~400 km from the camera).

Here the focus is on reported TLEs triggered by CG strokes matching with the superbolt criteria. Fig. 8a shows the 10.5-year superbolt

(a)

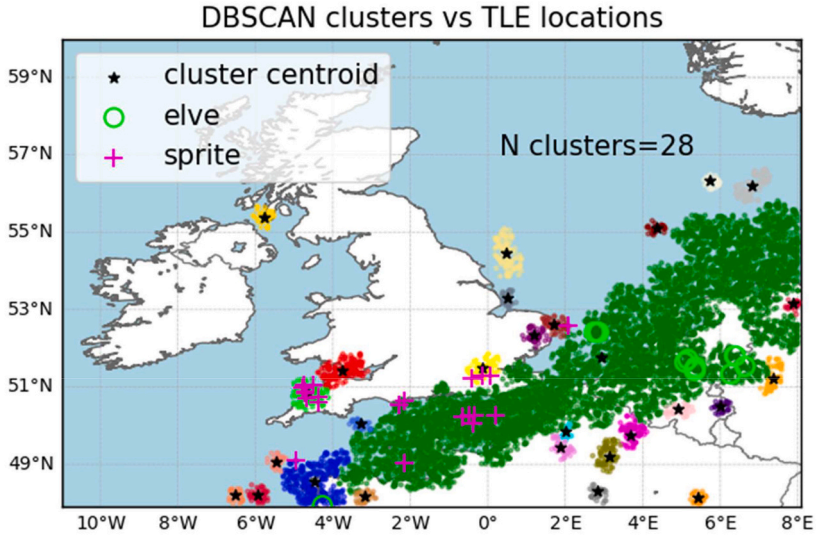

(b)

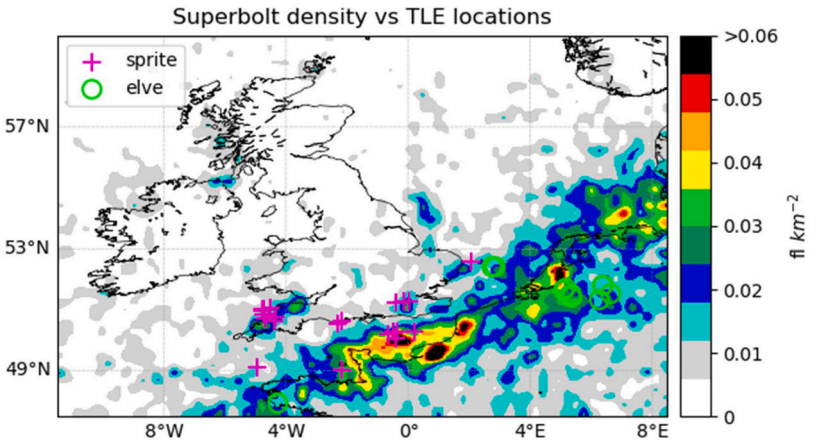

Fig. 8. (a) Distribution of TLE-associated superbolts with respect to the clusters identified with DBSCAN. The map shows that TLEs are not evenly distributed through the entire domain but, in general, tend to be confined to cluster boundaries in the southern region and in general where the superbolt density is larger than the overall average in the study area (b).

clusters and the corresponding locations of TLE parent CGs. While TLEs (notably sprites) related to lower peak current CGs have been observed throughout the entire domain, it is worth to notice that superbolt cluster boundaries are representative of the areas where the probability of eventually detecting an associated TLE is higher. As a result, the majority of observed TLEs related to superbolts is found on the sea or within few tens of kilometres inland from the coastline in the southern portion of the study area, where superbolt flash density increases with respect to the domain average (Fig. 8b). These have been observed throughout the year and in relation with different thunderstorm dynamics. A large number of sprites produced by superbolts has been already reported during an unusual late spring MCS in SW England (Pizzuti et al., 2021). An interesting case is that of winter superbolts occurring during peculiar thunderstorms observed in the UK that produce only few flashes per hour and occasionally trigger sprites. Since they tend to have the same polarity (often positive) and to be concentrated in a specific area and time of storm development, such strong flashes are potentially disruptive for power plants and airports giving the inherent sporadic onset. In the following section we analyse in more detail one of these cases during which concurrent sprites were optically captured.

3.3. Case study of 7th February 2016

Cold unstable airmass associated with a low-pressure system centred NW of Scotland reached the British Isles in the evening hours of 7th February 2016, and propagated eastwards across part of mainland UK overnight (Fig. 9). The frontal weather system with a dynamic wind field resulted in marginal thermodynamic instability with low topped convection along the frontal zone, as suggested by embedded bands of heavy rainfall (corresponding to radar reflectivity >50 dBZ, locally) derived from Met Office radar imagery (Fig. 10). Despite the relatively low minimum cloud top temperature (CTT) (~ − 45 °C at 23 UT), the presence of graupel and its motion, inferred by spectral width and Doppler velocity available from the Chilbolton 35-GHz radar (Copernicus), lead to convective invigoration and electrification with subsequent lightning onset at around 2250 UT, along the southern coast of England. The thunderstorm development was likely favoured by warmer and humid air advected from the English Channel as a consequence of the

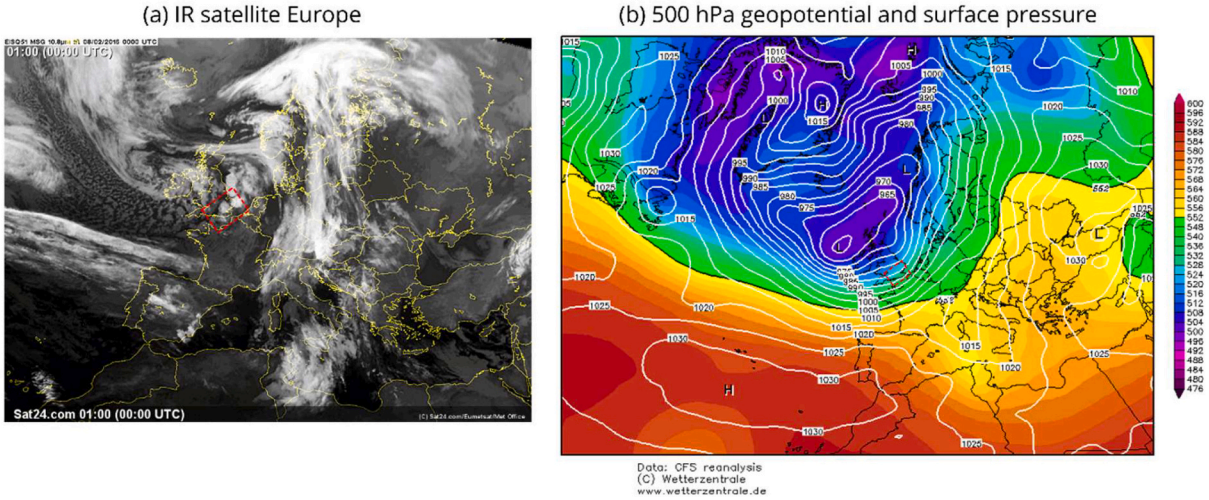

Fig. 9. Infrared (IR) satellite image (a), geopotential at 500 hPa and surface pressure plot issued from the Global Forecast System (GFS) model (b) for the 8th February 2016 at 0000 UT. The colormap scale is in decametres (dam). The dashed red frame indicates the investigated storm region. (For interpretation of the references to colour in this figure legend, the reader is referred to the web version of this article.)

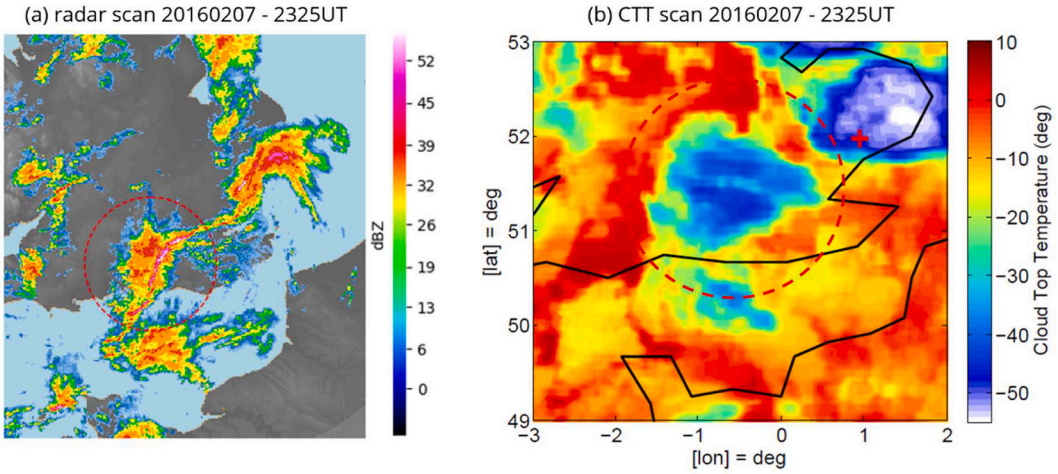

Fig. 10. Met Office Radar (a) and Meteosat cloud top temperature (CTT) (b) maps of the 7th February 2016 thunderstorm at about 2325UT, few minutes before the approximate time of first sprite onset. The region of interest is defined by the red dashed circle. The red cross indicates the location of a concurrent +CG stroke at about 23:26:01 UT, during the satellite scan and associated with a separate storm region. (For interpretation of the references to colour in this figure legend, the reader is referred to the web version of this article.)

low level south-westerly non-convective winds. Interestingly, the polarity of CG flashes detected by Météorage during electrically active periods was exclusively positive, which possibly allows making some hypotheses on charge configuration within the thundercloud (i.e. for example, the tilted positive dipole configuration, often observed during winter thunderstorms in Japan) (Nag and Rakov, 2012), though yet to be confirmed given the lack of electric field change measurements at ground under the storm. Electrical activity was rather weak (i.e., less than 10 CG flashes per hour detected and nearly absent IC activity in the period 2250 to 0000 UT) and limited in both time and space and underwent a substantial lull that culminated with the first sprite observation at about 2334 UT. Atmospheric soundings indicate that the 0 °C isotherm height was at ~1.1 km and the temperature at 700 hPa was ~ − 12.5 °C, in agreement with the criterion (<−10 °C) for winter lightning occurring in cold air mass thunderstorms used by Montanyà et al. (2016). The +CG flashes were located close behind the leading convective line, at about 30 km from the cold core of the cell which was around −50 °C at that time (Fig. 11). The total of 3 sprite events occurred in the onward half hour period at regular intervals of approximately 12 min from each other. Sprite development was quite unique in this case, as no other flashes were detected except those that triggered the sprites and the sprites themselves showed similar features, being classifiable as angel sprites (Bór, 2013) (Fig. 12). The absence of simultaneous electrical activity related to IC or other less intense CG in the preceding and following minutes around each event allowed for enough charge to build up and then be transferred to ground which enabled streamers development and propagation at mesospheric altitudes. The emergence of lateral streamers, typical of complex angel sprites, implies that the quasi-electrostatic field at sprite altitude, as a result of charge removal by the strong parent +CGs, is generally larger than that required for column sprites (Malagón-Romero et al., 2020). The 20 ms time resolution (de-interlaced) of available sprite videos do not allow tracking such a detailed evolution directly, but the approximate streamer initiation time within the sequence of the video fields agrees with the accepted temporal evolution (Fig. 13). The details and properties of the 3 sprite-parent +CGs are summarized in Table 1.

Fig. 14 shows the 100 Hz sampled quasi-electrostatic current detected at ELF frequency (1–50 Hz) on the Thunderstorm Detector (TD)

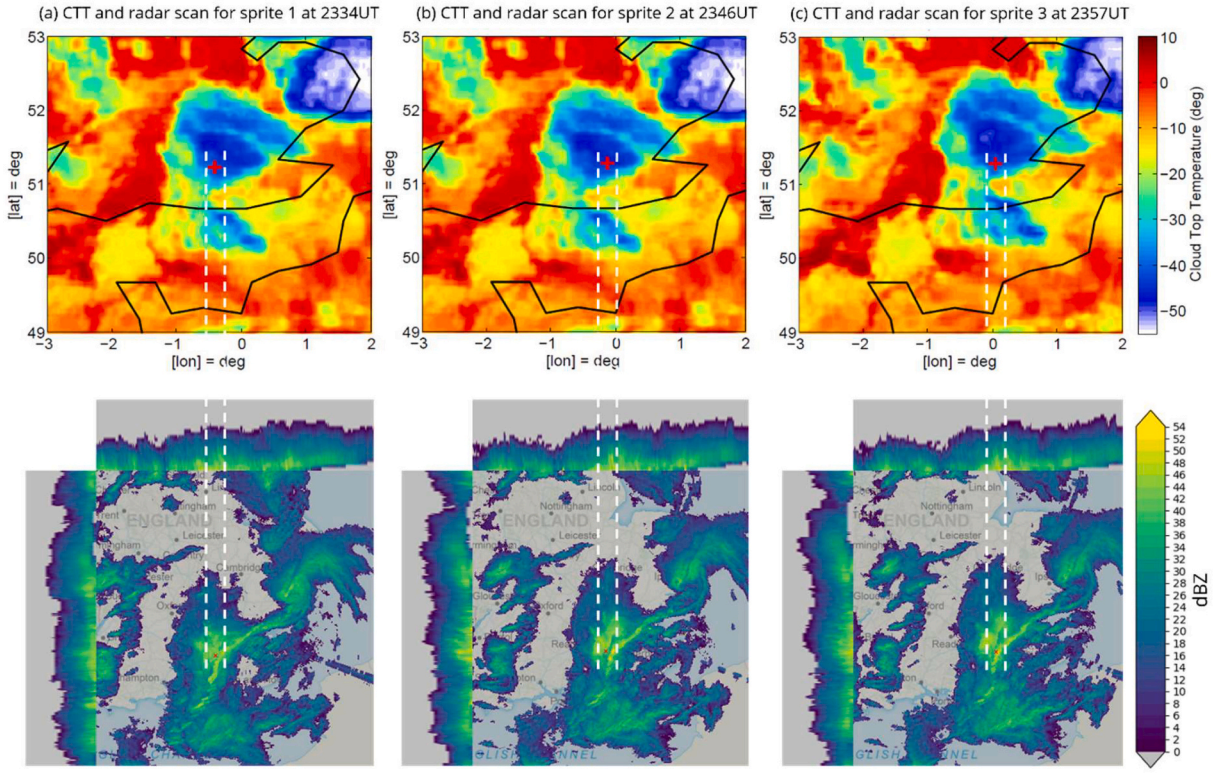

Fig. 11. Meteosat cloud top temperature (CTT) maps in the thermal infrared band (IR) (10.5–12.5 μm) and Met Office radar reflectivity (dBZ) at about 2334 UT (a), 2346 UT (b) and 2357 UT (c), corresponding to the 3 sprite events. The spatial resolution of radar maps is 1 km horizontally (central panel) and 500 m vertically, extending to an altitude of about 12 km (top and side panels). The sprite parent +CG (indicated by purple/red crosses on the maps) are located about 30 km south of the coldest (convective) core ~ −50 °C, for the three cases. The sprite locations trail behind a high radar reflectivity elongated band and it could indicate the direction of positive charge advected from the convective core. (For interpretation of the references to colour in this figure legend, the reader is referred to the web version of this article.)

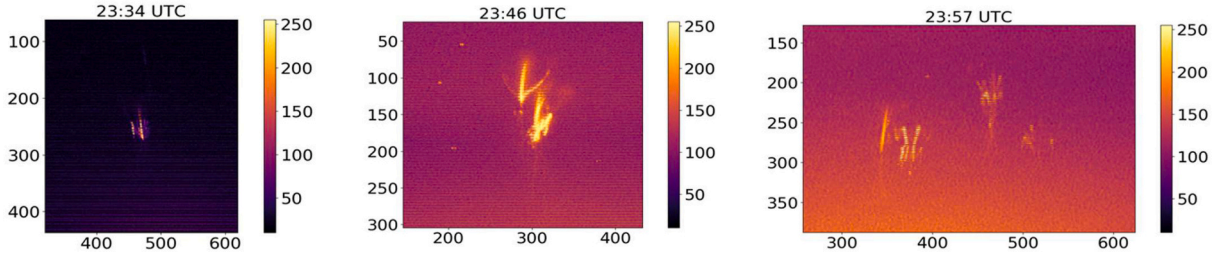

Fig. 12. The 3 sprites observed during the night of 7th/8th February 2016 (south London) between 2330 UT and 0000 UT, showing angel-sprite morphologies. (Courtesy: UKMON, Nemetode.org).

described by Bennett (2013) and installed at Reading (UK), at about 40 km from the sprite parent CG stroke locations. Sudden electric field changes related to the sprite parent +CG are visible as large amplitude signal with respect to the background. Since the TD is sensitive to all types of lightning within range, including weak IC, its raw output confirms the absence of other cloud or CG flashes in the area of interest during the half hour period starting from 2330 UT during which the sprites occurred. Simultaneous high-frequency (100 Hz) horizontal magnetic field recordings in the range 0.1–50 Hz were collected on two induction coil magnetometers at Eskdalemuir (UK). The North-South channel output, reported in the middle panel, shows the 3 sprite parent strokes in the magnetic field component and indicates a maximum peak-to-peak amplitude of ~530 pT for the event at 2357 UT. A further comparison with the electric field related signal detected on a BTD-300 (Bennett, 2017) installed at Portishead (UK), ~200 km away from the storm, shows a very good agreement with the magnetic data and highlights the idea that ELF flashes radiated by intense CG return strokes can be picked up at even larger distances using the same detection principle of the TD, when electrostatic field changes at ground following charge removal in lightning become negligible (Pizzuti et al., 2021). Additional lightning signals but associated with other active areas in the same period are also visible in the BTD output, as a result of the increased sensitivity with respect to the TD.

Early/fast events are lightning related disturbances in sub-ionospheric VLF radio transmissions (in amplitude and/or phase) that occur within 20 ms of the causative lightning and rise to full amplitude or phase change within the next 20 ms (Inan et al., 1996). They typically recover in 10–100 s or many minutes in some cases (Haldoupis et al., 2013; Koh et al., 2019), governed by the local chemical relaxation times in the ionosphere. These events have long been correlated with lightning, and more recently with sprites and TLEs in general (Inan et al., 1995; Dowden et al., 1996; Haldoupis et al., 2010). Such events are

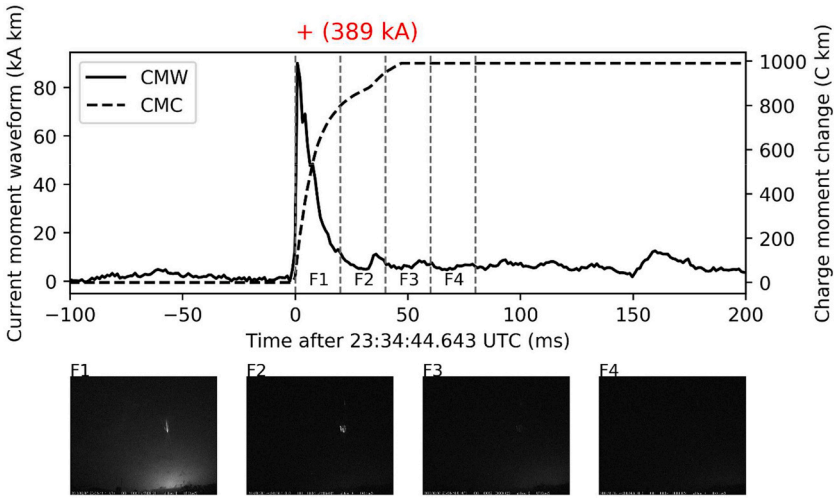

Fig. 13. Development of the first sprite at 23:33:44 UT on 7th February 2016: current moment waveform (CMW) with black curve, charge moment change (CMC) with dashed curve and peak current with red plus, of the causative +CG stroke. The images of the sprite correspond to 20 ms fields obtained by de-interlacing the video frames. (For interpretation of the references to colour in this figure legend, the reader is referred to the web version of this article.)

Table 1
List of sprite-parent +CGs.

Date	Time (UTC)	Lat	Lon	Peak current (kA)	iCMC (C km)	CMC (C km)
2016-02-07	23:34:44.643	51.236	−0.4016	+389	+172	+990
2016-02-07	23:46:46.499	51.2839	−0.1238	+295	+127	+829
2016-02-07	23:57:18.319	51.2748	0.0528	+393	+174	+1307

detected because the VLF transmitter signal received is highly sensitive to the local ionospheric conductivity, which is affected by modifications in the electron density or collision frequency (through heating and ionization). The perturbation parameters are function of the relative distances between the lightning and eventually associated TLE and the great circle path between transmitter and receiver (NaitAmor et al., 2010). At the time of sprite observations, one of such narrowband VLF receiver was operating at Algiers, monitoring at 20 ms time resolution the VLF signal from various transmitters located globally. On this favourable occasion, the great circle path between the receiver and the GQD transmitter (22.1 kHz) approximately crossed the sprite region. The data in Fig. 15 indicate that all the 3 superbolts and subsequent sprites observed in the UK were the sources of early signal perturbations in the GQD-Algiers transmission path. The type of perturbation recorded belongs to the class of LOREs (LOng Recovery Early VLF events) with >200 s recovery times, documented by Haldoupis et al. (2012). In particular, the first event at 23:34:44 UT is found to recover to the level preceding the lightning flash in about 6 min. The other two events at 23:46:46 UT and 23:57:18 UT show similar features to step-like LOREs described by Haldoupis et al. (2013), exhibiting even larger recovery times or no recovery. The onset of LOREs may indirectly suggest the existence of elves preceding the observed sprites, as a result of the strong EMP radiated by such large peak current +CG and its interaction with the lower ionosphere. No concurrent effects were recorded on NRK and DHO paths, because of the significantly larger distance from the storm centre.

4. Discussion

We have presented details of ~15,000 very large peak current (i.e. about 10 times larger than average values) strokes for 2010–2020 in a spatial domain centred on the British Isles. These strokes have seasonal and geographic distributions that match with the patterns of superbolts observed by Holzworth et al. (2019) in the same area, suggesting that a significant proportion of events selected using the peak current criteria may actually coincide with superbolts detected by WWLLN and classified in terms of radiated VLF energy over 10^6 J. Flash density calculations and clustering of the superbolt locations by means of DBSCAN algorithm allowed us to identify the areas of larger concentration of these events with increased resolution and to highlight the different patterns observed by considering additional properties, such as the stroke polarity. The cluster positions are found to vary through the year in agreement with the dominant seasonal weather patterns and the corresponding lightning occurrence distributions that affect Britain and surrounding areas (Wilkinson and Neal, 2021). An interesting case for the UK is that of low active convective storms during the winter season, which produce one or few CG flashes per hour over a limited size area. On these occasions, large peak current CGs are often the predominant type of lightning observed. They usually occur in rapid succession and are delimited to a specific area and time of the storm development, as seen in section 3.3, when about 72% of the total CGs occurred in the period examined exceeded 100 kA and half of this population of strong CGs were superbolts.

Observations in this study further confirm that the most intense superbolts are preferentially found over the sea or along the coastlines (e.g., Füllekrug et al., 2002), as indicated by the most populated cluster stretching from the English Channel to the coast of the Netherlands. The large cluster on the English Channel persists during the winter season (NDJF) but is largely dominated by negative polarity strokes with a peak at early morning hours. The SW-NE orientation of the English Channel favours enhancement of wintertime convection during the unstable conditions resulting from both SW and NE airflow (Galvin, 2021), both of which are common wind directions for the region. For the case of an unstable wintertime SW airflow, convection initiated over the sea within the returning Polar Maritime air mass is enhanced in the channel by low-level convergence resulting from the backing of wind due to friction over the rougher land surface of France (Gille and Llewellyn Smith, 2014). Similarly, convection in an unstable NE Polar Maritime air mass will be enhanced in the channel by low-level convergence of airflow backed over the relatively rougher land surface of England. This enhanced

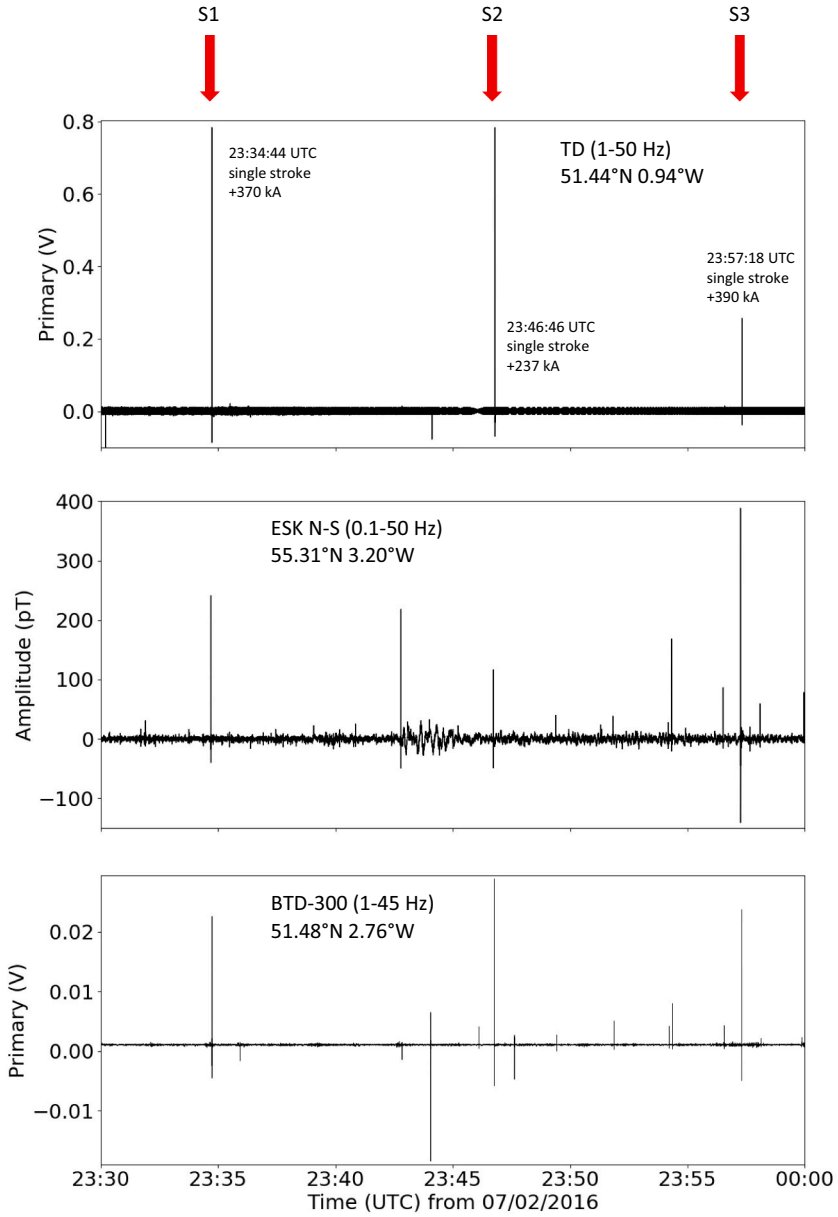

Fig. 14. Monitoring of electrical and magnetic activity during the interval 2330/0000 UT, when the sprites occurred (indicated by the red arrows and labelled as S1, S2 and S3, respectively), in the ELF band (<50 Hz). The signals associated with the strong parent strokes were clearly detected in both the components at various distances from the stroke locations. The TD (the closest to the storm centre, <50 km) output also confirms the absence of concurrent electrical activity around the time of each event, except for the +CGs that triggered the sprites. (For interpretation of the references to colour in this figure legend, the reader is referred to the web version of this article.)

convergence in the Channel would increase the probability of convective initiation and deepen existing convective cloud, thereby increasing winter lightning occurrence on that stretch of sea. Given the proximity between the superbolt cluster and one of the most congested maritime routes in Europe (Fig. 16), we cannot exclude that, while atmospheric instability and vertical updrafts enhanced by low-level convergence are the dominant factors determining lightning activity, advected aerosols from the sea and shipping lanes in winter conditions may act as a modulating factor in the ice microphysics leading to intensification of convection and storm electrification and consequently in lightning enhancement (e.g., Lyons et al., 1998; Altaratz et al., 2010; Thornton et al., 2017; Yair, 2018; Yair et al., 2021). Higher concentrations of cloud condensation nuclei (CCN) have been found to lead to enhanced updrafts (Mansell and Ziegler, 2013) and an increase of supercooled droplets reaching the mixed-phase region of the cloud, culminating in a more effective charge separation and cloud electrification (Deierling et al., 2008). Various physical mechanisms may act in concert to determine the large proportion of high peak current strokes and the observed polarity disparity, biased towards negative superbolts across the area. In a recent experiment, Asfur et al. (2020) hypothesized that the higher conductivity of the saline water, compared to moist soil, results in a more efficient charge transfer to the surface and subsequently in larger peak current discharges and brighter optical flashes. On the other hand, Cooray and Rakov (2012) described a formula to predict the peak current in first negative return strokes as a function of either the potential difference between the cloud charge region and the ground or the background electric field, that is theoretically limited to a maximum value of about 150 kV/m. In general, this background electric field will not be reduced over open water, given the decreased opportunity for corona (point) discharge and absence of upward leaders from tall structures on ground, thereby favouring a larger maximum return stroke peak current attainable with respect to land-based thunderstorms. Another possible explanation for the predominance of large peak current -CGs reported by lightning location systems on the English Channel is the faster average vertical velocity of negative first stroke leaders propagating downward over the ocean, as reported by Nag and Cummins (2017). If confirmed by future observations, this mechanism would also allow to make specific assumption on the charge configuration of

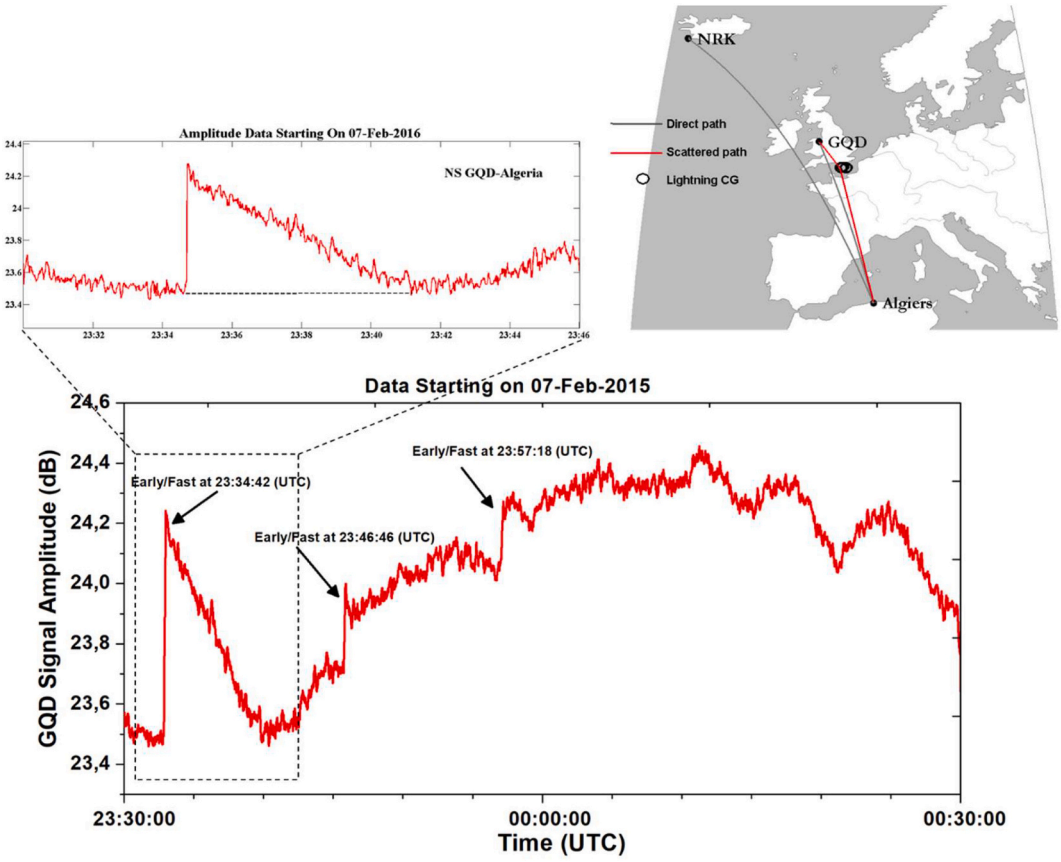

Fig. 15. Long recovery and step-like early/fast VLF signal perturbations associated with the large peak current sprite-parent +CG in the UK and recorded by the receiver in Algiers. An approximate geometry of the transmitter–receiver paths is shown in the map.

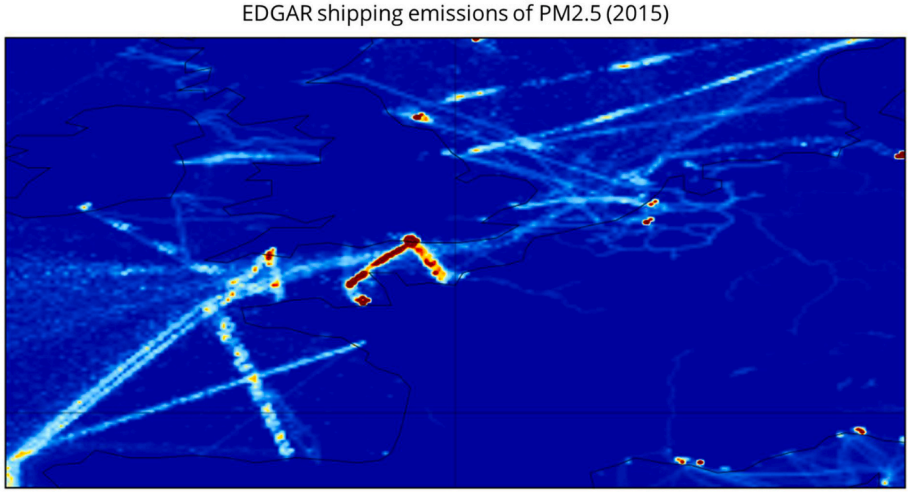

Fig. 16. Map of shipping emissions in the study area using data from EDGAR (Emissions Database for Global Atmospheric Research) for the year 2015, showing the largest concentrations of $PM_{2.5}$ particles on the English Channel.

maritime thunderstorms producing negative superbolts, such as large main negative charge region and small or absent lower positive charge layer. In particular, the development of lower positive charge region would be inhibited over the water surface by the decreased upward transport of positive charge produced by corona effect at ground and the presence of traces of NaCl in maritime air, which leads to negative charge on graupel irrespective of temperature in the graupel-ice collision mechanism (e.g., Cooray and Rakov, 2012, and references therein).

We additionally reported evidence that winter storms producing superbolts in the study area, despite the low electrical activity and limited size extent, can be capable of triggering sprites, as in the unique case described of 7th Feb, 2016, when 3 sprites coincided with the only 3 + CG strokes occurred in an half hour interval of the storm evolution. Various studies have shown that winter weather regimes and cloud properties, determining low IC rate thunderstorms on the sea and coastal areas of Atlantic Europe (e.g. the Bay of Biscay), are prolific producers of large peak current CG strokes of either polarity and associated elves (Van der Velde et al., 2011), but only rarely produce sprites, whose

activity is generally limited to the Mediterranean during winter (Yair et al., 2015; Arnone et al., 2020). The key factor for the formation of sprites is the magnitude of the vertical CMC of parent +CG stroke (Hu et al., 2002) and the subsequent rapid change in the above-cloud quasi-electrostatic (QE) field. CMC values estimated for the sprite-parent strokes in this study are found to be in the range of average values of 1400 ± 600C km for winter thunderstorms reported by Yair et al. (2009). An additional more stringent metric than the return stroke peak current to evaluate the sprite-producing potential of lightning strokes is the iCMC, defined as the total CMC within the first 2 ms after the lightning return stroke. Lu et al. (2013) observed a 90% likelihood for +CG strokes with a mean iCMCs > +300C km to produce a sprite, which is considerably lower than the mean iCMC value of +571C km associated with halo-sprite events (Lu et al., 2018). An extensive survey on iCMC measurements across the U.S. by Cummer et al. (2013) analysed the relationship between the peak current and the iCMC, showing that the distribution for very high peak current positive strokes (> +200 kA) is peaked at very low iCMC (~ + 20C km) and substantially drops for larger values, thus implying positive superbolts as a not favourable sprite-producing source. If the same distribution is assumed to be valid also for positive superbolts occurring in the study area, the sprite observations here described are therefore rather atypical events. By contrast, the measurements reported by Cummer et al. (2013) show an opposite result for negative CG strokes, indicating that the peak in the iCMC distribution increases with the return stroke peak current and a significant spread of the distribution for large peak current -CG (<−200 kA). This may suggest an increased potential for negative superbolts over open water (such as the English Channel) to result in mesospheric halos (Frey et al., 2007) that, however, needs to be supported by future observational campaigns. A significant discrepancy is found between the winter sprites observed during the night of 7th/8th Feb, 2016, associated with relatively small iCMCs (e.g., below +200C km), and the other documented cases of sprites observed above a rare late spring MCS in the UK, characterised by similarly high peak current values but a mean iCMC of about +680C km (Pizzuti et al., 2021). This can be reasonably attributed to relevant differences in cloud properties, such as the thundercloud charge and electric field configuration, and the subsequent details of charge transfer in the CG strokes. Yet, modification of atmospheric medium in response to sequential strong electromagnetic pulses emitted by superbolts may contribute to the emergence of short time delayed sprites associated with parent +CGs exhibiting smaller iCMCs. Haldoupis et al. (2013) showed that intense ±CG with peak currents >200 kA in absolute value cause long-lasting (e.g., many minutes) ionization changes in the lower nighttime ionosphere, resulting in detectable long-recovery perturbations on man-made VLF transmissions, as shown by VLF measurements in this study. Salut et al. (2013) also reported that the number of long-recovery (>500 s) early VLF events increases with the peak current of CG return, especially when occurring over the sea, although Kotovsky et al. (2016) argued that the intense initial breakdown observed in lightning producing LOREs do not necessarily imply the involvement of high peak currents and large electromagnetic pulse radiation in producing the long-lived ionospheric disturbance. According to theoretical models (e.g., Taranenko et al., 1993; Marshall, 2012), the interaction of lightning EMP with the lower ionosphere results in electron density enhancement by impact ionization above ~85 km and electron density depletion due to electron attachment at lower altitudes (e.g., below about 80 to 85 km). The sharp steepening of the ambient electron density by consecutive strong CG may thus have a direct concurrent effect on the initiation of sprite streamers, in combination with the CMC of the parent +CG (Qin et al., 2011; Qin et al., 2012).

5. Conclusions

This study provides the first detailed climatology of superbolts in the region of northwestern Europe that comprises the British Isles, enabling further comparisons with previous studies and setting the basis for new research. We conclude that, in addition to relevant discrepancies found between the distribution of positive and negative superbolts, 1) superbolts occurring at this latitude can be a potential source of TLEs (especially elves and halos), such as under weather patterns typical of winter season, thus deserving further investigation on specific properties of lightning inception and leader propagation characteristics, 2) convergence and advection of salt water aerosols and shiptrack emissions over the English Channel may effectively contribute to convective invigoration and the development of cloud charge configurations favouring such extreme events, during nearly zero flash rate marginal thunderstorms, 3) the identification of highly populated superbolt regions via clustering methods may be useful to target new observational campaigns in this part of Europe which is normally out of range of most of European TLEs observation networks.

CRediT authorship contribution statement

Andrea Pizzuti: Writing – original draft, Writing – review & editing, Conceptualization, Investigation, Formal analysis. **Alec Bennett:** Conceptualization, Methodology, Validation, Supervision. **Serge Soula:** Resources, Formal analysis. **Samir Nait Amor:** Resources, Formal analysis. **Janusz Mlynarczyk:** Resources, Formal analysis. **Martin Füllekrug:** Conceptualization, Supervision. **Stéphane Pédeboy:** Resources.

Declaration of Competing Interest

The authors declare no conflict of interest. The funders had no role in the design of the study; in the collection, analyses, or interpretation of data; in the writing of the manuscript, or in the decision to publish the results.

Acknowledgments

This research has received funding from the European Union's Horizon 2020 research and innovation programme under the Marie Sklodowska-Curie grant agreement 722337. JM acknowledges support from the National Science Centre, Poland, under grant 2015/19/B/ST10/01055. The authors are grateful to the UKMON and NEMETODE, for providing the database and imagery of sprites used in the study, to Ciaran Beggan (British Geological Survey), for the high frequency magnetic field induction coil data from Eskdalemuir Observatory, UK, and to the UK Met Office, in particular Robert Scovell and Jonathan Wilkinson, for providing the radar reflectivity maps.

References

Adachi, T., Fukunishi, H., Takahashi, Y., Sato, M., Ohkubo, A., Yamamoto, K., 2005. Characteristics of thunderstorm systems producing winter sprites in Japan. J. Geophys. Res.-Atmos. 110 (D11).
Altaratz, O., Koren, I., Yair, Y., Price, C., 2010. Lightning response to smoke from Amazonian fires. Geophys. Res. Lett. 37 (7).
Aminou, D.M.A., Jacquet, B., Pasternak, F., 1997, December. Characteristics of the Meteosat Second Generation (MSG) radiometer/imager: SEVIRI. In: Sensors, Systems, and Next-Generation Satellites, vol. 3221. International Society for Optics and Photonics, pp. 19–31.
Anderson, G., Klugmann, D., 2014. A European lightning density analysis using 5 years of ATDnet data. Nat. Hazards Earth Syst. Sci. 14 (4), 815–829.
Arnone, E., Bór, J., Chanrion, O., Barta, V., Dietrich, S., Enell, C.F., Neubert, T., 2020. Climatology of transient luminous events and lightning observed above Europe and the Mediterranean Sea. Surv. Geophys. 41 (2), 167–199.
Asfur, M., Price, C., Silverman, J., Wishkerman, A., 2020. Why is lightning more intense over the oceans? J. Atmos. Sol. Terr. Phys. 202, 105259.
Beggan, C.D., Musur, M., 2018. Observation of ionospheric Alfvén resonances at 1–30 Hz and their superposition with the Schumann resonances. J. Geophys. Res. Space Physics 123 (5), 4202–4214.
Bennett, A.J., 2013. Identification and ranging of lightning flashes using co-located antennas of different geometry. Meas. Sci. Technol. 24 (12), 125801.
Bennett, A.J., 2017. Electrostatic thunderstorm detection. Weather 72 (2), 51–54.

Blanc, E., Farges, T., Brebion, D., Belyaev, A.N., Alpatov, V.V., Labarthe, A., Melnikov, V., 2007. Main results of LSO (Lightning and Sprite Observations) on board of the International Space Station. Microgravity Sci. Technol. 19 (5), 80–84.
Bór, J., 2013. Optically perceptible characteristics of sprites observed in Central Europe in 2007–2009. J. Atmos. Sol. Terr. Phys. 92, 151–177.
Cooray, V., Rakov, V., 2012. On the upper and lower limits of peak current of first return strokes in negative lightning flashes. Atmos. Res. 117, 12–17.
Cummer, S.A., Lyons, W.A., Stanley, M.A., 2013. Three years of lightning impulse charge moment change measurements in the United States. J. Geophys. Res.-Atmos. 118 (11), 5176–5189.
Deierling, W., Petersen, W.A., Latham, J., Ellis, S., Christian, H.J., 2008. The relationship between lightning activity and ice fluxes in thunderstorms. J. Geophys. Res.-Atmos. 113 (D15).
Dowden, R.L., Brundell, J.B., Lyons, W.A., Nelson, T., 1996. Detection and location of red sprites by VLF scattering of subionospheric transmissions. Geophys. Res. Lett. 23 (14), 1737–1740.
Ester, M., Kriegel, H.P., Sander, J., Xu, X., 1996, August. A density-based algorithm for discovering clusters in large spatial databases with noise. In: Proceedings of the Second International Conference on Knowledge Discovery and Data Mining (KDD-96). AAAI Press, pp. 226–231.
Frey, H.U., Mende, S.B., Cummer, S.A., Li, J., Adachi, T., Fukunishi, H., Chang, Y.S., 2007. Halos generated by negative cloud-to-ground lightning. Geophys. Res. Lett. 34 (18).
Füllekrug, M., Price, C., Yair, Y., Williams, E.R., 2002, January. Letter to the Editor Intense oceanic lightning. Ann. Geophys. 20 (1), 133–137. Copernicus GmbH.
Galvin, J., 2021. Convergence line in the English Channel. Weather 76 (5), 173–174.
Gille, S.T., Llewellyn Smith, S.G., 2014. When land breezes collide: converging diurnal winds over small bodies of water. Q. J. R. Meteorol. Soc. 140 (685), 2573–2581.
Haldoupis, C., Amvrosiadi, N., Cotts, B.R.T., Van der Velde, O.A., Chanrion, O., Neubert, T., 2010. More evidence for a one-to-one correlation between Sprites and Early VLF perturbations. J. Geophys. Res. Space Physics 115 (A7).
Haldoupis, C., Cohen, M., Cotts, B., Arnone, E., Inan, U., 2012. Long-lasting D-region ionospheric modifications, caused by intense lightning in association with elve and sprite pairs. Geophys. Res. Lett. 39 (16).
Haldoupis, C., Cohen, M., Arnone, E., Cotts, B., Dietrich, S., 2013. The VLF fingerprint of elves: Step-like and long-recovery early VLF perturbations caused by powerful ±CG lightning EM pulses. J. Geophys. Res. Space Physics 118 (8), 5392–5402.
Hayakawa, M., Nakamura, T., Hobara, Y., Williams, E., 2004. Observation of sprites over the Sea of Japan and conditions for lightning-induced sprites in winter. J. Geophys. Res. Space Physics 109 (A1).
Holzworth, R.H., McCarthy, M.P., Brundell, J.B., Jacobson, A.R., Rodger, C.J., 2019. Global distribution of superbolts. J. Geophys. Res.-Atmos. 124 (17–18), 9996–10005.
Hu, W., Cummer, S.A., Lyons, W.A., Nelson, T.E., 2002. Lightning charge moment changes for the initiation of sprites. Geophys. Res. Lett. 29 (8), 120–121.
Hutchins, M.L., Holzworth, R.H., Rodger, C.J., Brundell, J.B., 2012. Far-field power of lightning strokes as measured by the World Wide Lightning Location Network. J. Atmos. Ocean. Technol. 29 (8), 1102–1110.
Inan, U.S., Bell, T.F., Pasko, V.P., Sentman, D.D., Wescott, E.M., Lyons, W.A., 1995. VLF signatures of ionospheric disturbances associated with sprites. Geophys. Res. Lett. 22 (24), 3461–3464.
Inan, U.S., Slingeland, A., Pasko, V.P., Rodriguez, J.V., 1996. VLF and LF signatures of mesospheric/lower ionospheric response to lightning discharges. J. Geophys. Res. Space Physics 101 (A3), 5219–5238.
Kirkland, M.W., 1999. An Examination of Superbolt-Class Lightning Events Observed by the FORTE Satellite. Los Alamos National Laboratory, Atmospheric Sciences Group, New Mexico.
Koh, K., Bennett, A., Ghilain, S., Liu, Z., Pedeboy, S., Peverell, A., Füllekrug, M., 2019. Lower ionospheric conductivity modification above a thunderstorm updraught. J. Geophys. Res. Space Physics 124 (8), 6938–6949.
Kotovsky, D.A., Moore, R.C., Zhu, Y., Tran, M.D., Rakov, V.A., Pilkey, J.T., Uman, M.A., 2016. Initial breakdown and fast leaders in lightning discharges producing long-lasting disturbances of the lower ionosphere. J. Geophys. Res. Space Physics 121 (6), 5794–5804.
Kriegel, H.P., Kröger, P., Sander, J., Zimek, A., 2011. Density-based clustering. Wiley Interdisc. Rev.: Data Mining Knowledge Discovery 1 (3), 231–240.
Kulak, A., Kubisz, J., Klucjasz, S., Michalec, A., Mlynarczyk, J., Nieckarz, Z., Zieba, S., 2014. Extremely low frequency electromagnetic field measurements at the Hylaty station and methodology of signal analysis. Radio Sci. 49 (6), 361–370.
Lu, G., Cummer, S.A., Li, J., Zigoneanu, L., Lyons, W.A., Stanley, M.A., Samaras, T., 2013. Coordinated observations of sprites and in-cloud lightning flash structure. J. Geophys. Res.-Atmos. 118 (12), 6607–6632.
Lu, G., Yu, B., Cummer, S.A., Peng, K.M., Chen, A.B., Lyu, F., Su, H.T., 2018. On the causative strokes of halos observed by ISUAL in the vicinity of North America. Geophys. Res. Lett. 45 (19), 10–781.
Lyons, W.A., Nelson, T.E., Williams, E.R., Cramer, J.A., Turner, T.R., 1998. Enhanced positive cloud-to-ground lightning in thunderstorms ingesting smoke from fires. Science 282 (5386), 77–80.
Malagón-Romero, A., Teunissen, J., Stenbaek-Nielsen, H.C., McHarg, M.G., Ebert, U., Luque, A., 2020. On the emergence mechanism of carrot sprites. Geophys. Res. Lett. 47 (1) e2019GL085776.
Mansell, E.R., Ziegler, C.L., 2013. Aerosol effects on simulated storm electrification and precipitation in a two-moment bulk microphysics model. J. Atmos. Sci. 70 (7), 2032–2050.
Mäkelä, A., Kantola, T., Yair, Y., Raita, T., 2010. Observations of TLEs above the Baltic sea on Oct 9 2009. Geophysica 46 (1–2), 79–90.
Marshall, R.A., 2012. An improved model of the lightning electromagnetic field interaction with the D-region ionosphere. J. Geophys. Res. Space Physics 117 (A3).
Mlynarczyk, J., Bór, J., Kulak, A., Popek, M., Kubisz, J., 2015. An unusual sequence of sprites followed by a secondary TLE: an analysis of ELF radio measurements and optical observations. J. Geophys. Res. Space Physics 120 (3), 2241–2254.
Montanyà, J., Fabró, F., Velde, O.V.D., March, V., Williams, E.R., Pineda, N., Freijo, M., 2016. Global distribution of winter lightning: a threat to wind turbines and aircraft. Nat. Hazards Earth Syst. Sci. 16 (6), 1465–1472.
Nag, A., Cummins, K.L., 2017. Negative first stroke leader characteristics in cloud-to-ground lightning over land and ocean. Geophys. Res. Lett. 44 (4), 1973–1980.
Nag, A., Rakov, V.A., 2012. Positive lightning: an overview, new observations, and inferences. J. Geophys. Res.-Atmos. 117 (D8).
NaitAmor, S., Al Abdoadaim, M.A., Cohen, M.B., Cotts, B.R.T., Soula, S., Chanrion, O., Abdelatif, T., 2010. VLF observations of ionospheric disturbances in association with TLEs from the EuroSprite-2007 campaign. J. Geophys. Res. Space Physics 115 (A7).
Pasko, V.P., 2010. Recent advances in theory of transient luminous events. J. Geophys. Res. Space Physics 115 (A6).
Pasko, V.P., Yair, Y., Kuo, C.L., 2012. Lightning related transient luminous events at high altitude in the Earth's atmosphere: phenomenology, mechanisms and effects. Space Sci. Rev. 168 (1), 475–516.
Pedeboy, S., Bernardi, M., Schulz, W., Rousseau, A., 2017. Characteristics and distribution of intense cloud-to-ground flashes in Western Europe. In: *International Colloquium on Lightning and Power Systems*, Ljubljana (Slovenia).
Pédeboy, S., Barnéoud, P., Defer, E., Coquillat, S., 2018. Analysis of the intra-cloud lightning activity detected with low frequency lightning locating systems. In: 25th International Lightning Detection Conference, 7th International Lightning Meteorology Conference, pp. 12–15.
Peterson, M., Kirkland, M.W., 2020. Revisiting the detection of optical lightning superbolts. J. Geophys. Res.-Atmos. 125 (23) e2020JD033377.
Pizzuti, A., Wilkinson, J.M., Soula, S., Mlynarczyk, J., Kolmašová, I., Santolík, O., Füllekrug, M., 2021. Signatures of large peak current lightning strokes during an unusually intense sprite-producing thunderstorm in southern England. Atmos. Res. 249, 105357.
Qin, J., Celestin, S., Pasko, V.P., 2011. On the inception of streamers from sprite halo events produced by lightning discharges with positive and negative polarity. J. Geophys. Res. Space Physics 116 (A6).
Qin, J., Celestin, S., Pasko, V.P., 2012. Minimum charge moment change in positive and negative cloud to ground lightning discharges producing sprites. Geophys. Res. Lett. 39 (22).
Ripoll, J.F., Farges, T., Malaspina, D.M., Cunningham, G.S., Lay, E.H., Hospodarsky, G.B., Pédeboy, S., 2021. Electromagnetic power of lightning superbolts from Earth to space. Nat. Commun. 12 (1), 1–10.
Salut, M.M., Cohen, M.B., Ali, M.A.M., Graf, K.L., Cotts, B.R.T., Kumar, S., 2013. On the relationship between lightning peak current and early VLF perturbations. J. Geophys. Res. Space Physics 118 (11), 7272–7282.
Schulz, W., Diendorfer, G., Pedeboy, S., Poelman, D.R., 2016. The European lightning location system EUCLID–Part 1: performance analysis and validation. Nat. Hazards Earth Syst. Sci. 16 (2), 595–605.
Takahashi, Y., Miyasato, R., Adachi, T., Adachi, K., Sera, M., Uchida, A., Fukunishi, H., 2003. Activities of sprites and elves in the winter season, Japan. J. Atmos. Sol. Terr. Phys. 65 (5), 551–560.
Taranenko, Y.N., Inan, U.S., Bell, T.F., 1993. Interaction with the lower ionosphere of electromagnetic pulses from lightning: heating, attachment, and ionization. Geophys. Res. Lett. 20 (15), 1539–1542.
Taylor, S., Stier, P., White, B., Finkensieper, S., Stengel, M., 2017. Evaluating the diurnal cycle in cloud top temperature from SEVIRI. Atmos. Chem. Phys. 17 (11), 7035–7053.
Thornton, J.A., Virts, K.S., Holzworth, R.H., Mitchell, T.P., 2017. Lightning enhancement over major oceanic shipping lanes. Geophys. Res. Lett. 44 (17), 9102–9111.
Turman, B.N., 1977. Detection of lightning superbolts. J. Geophys. Res. 82 (18), 2566–2568.
Van der Velde, O.A., Montañá Puig, J., Fullekrug, M., Soula, S., 2011. Gravity waves, meteor trails and asymmetries in elves. In: Special Issue: 14th International Conference on Atmospheric Electricity, held in Rio de Janeiro (August 8–12, 2011). Elsevier, pp. 1–4.
Wilkinson, J.M., Neal, R., 2021. Exploring relationships between weather patterns and observed lightning activity for Britain and Ireland. Q. J. R. Meteorol. Soc. 147, 2772–2795.
Yair, Y., 2018. Lightning hazards to human societies in a changing climate. Environ. Res. Lett. 13 (12), 123002.
Yair, Y., Price, C., Ganot, M., Greenberg, E., Yaniv, R., Ziv, B., Sátori, G., 2009. Optical observations of transient luminous events associated with winter thunderstorms near the coast of Israel. Atmos. Res. 91 (2–4), 529–537.
Yair, Y., Price, C., Katzenelson, D., Rosenthal, N., Rubanenko, L., Ben-Ami, Y., Arnone, E., 2015. Sprite climatology in the Eastern Mediterranean Region. Atmos. Res. 157, 108–118.
Yair, Y., Lynn, B., Ziv, B., Yaffe, M., 2020, May. Lightning super-bolts in Eastern Mediterranean winter thunderstorms. In: EGU General Assembly Conference Abstracts, p. 1788.
Yair, Y., Price, C., Namia-Cohen, Y., Lynn, B., Shpund, J., Yaffe, M., 2021, April. Why are lightning super-bolts more frequent in East Mediterranean winter thunderstorms?. In: EGU General Assembly Conference Abstracts EGU21-1474.